9-1-2003

Thermal Properties of $La_{0.5}Sr_{0.5}Co_{1-x}NixO_3\text{-d}$ Ceramics using Photopyroelectric Technique

M. T. Sebastian

C. Preethy Menon

J. Philip

Robert W. Schwartz
Missouri University of Science and Technology

Recommended Citation

Thermal properties of $La_{0.5}Sr_{0.5}Co_{1-x}Ni_xO_{3-\delta}$ ceramics using photopyroelectric technique

M. T. Sebastian[a)]
Regional Research Laboratory, Trivandrum-695 019, India

C. Preethy Menon and J. Philip
Department of Instrumentation, Cochin University of Science & Technology, Cochin-682 022, India

R. W. Schwartz
Department of Ceramic Engineering, University of Missouri-Rolla, Rolla, Missouri

$La_{0.5}Sr_{0.5}Co_{1-x}Ni_xO_{3-\delta}$ ($0 \leq x \leq 0.6$) ceramics were prepared using a conventional solid-state ceramic route. The thermal properties—thermal conductivity and heat capacity—of these ceramics were measured by the photopyroelectric technique. The thermal conductivity was found to increase with increasing Ni content. These materials were also found to exhibit a metallic-type variation of thermal conductivity with temperature, and no metal-insulator (M-I) transition was found to occur in any of the samples prepared by this route. However, a M-I transition was found to occur in $La_{0.5}Sr_{0.5}CoO_{3-\delta}$ samples prepared by hot pressing. The difference is attributed to variations in oxygen content in the samples. © *2003 American Institute of Physics.* [DOI: 10.1063/1.1598628]

I. INTRODUCTION

Currently there is considerable interest in the chemical and physical properties of lanthanum strontium cobaltate ceramics with the general formula $La_{0.5}Sr_{0.5}CoO_3$ (LSCO) due to their potential applications in the fields of catalysis[1,2] dense ceramic membranes,[3] gas sensors,[4,5] oxide fuel cell electrodes,[6–8] electrodes for ferroelectric memory devices[9,10] and giant magneto-resistance devices.[11–13] LSCO ceramics are widely used as electrode materials because of their isotropic low electrical resistivity[14,15] and good chemical stability. The resistivity of (001) oriented LSCO thin films is in the range of 130–200 $\mu\Omega$ cm, whereas in the bulk it is about 90 $\mu\Omega$ cm.[16] It has been reported that substitution of Sr^{2+} for La^{3+} in $LaCoO_3$ brings about remarkable changes in the system, such as a metal-insulator transition,[17] change in crystal structure,[18] etc. It is found that lattice distortion and electrical resistivity of this material increase with increasing strontium content.

The pseudo cubic lattice constant of LSCO ($3.83A^0$) closely matches many ferroelectric materials of interest. Recently, LSCO perovskites have been reported as a very suitable electrode material[10,19–21] that is capable of providing superior fatigue and imprint resistance in ferroelectric thin film devices. The reason for the superior performance of devices based on conductive LSCO perovskite electrodes is that they are compatible with perovskite ferroelectrics both chemically and crystallographically. The use of an LSCO cathode in a sealed-off CO_2 laser was found to improve the performance of the laser in both output power and operating life.[4,5,22] LSCO is nonstoichiometric and the nonstoichiometry parameter δ increases with strontium content (x) and

increasing temperature or decreasing oxygen partial pressure.[23] More recently, Schwartz *et al.*[24,25] have found that partial substitution of Co by Ni (LSCNO) increases the electrical conductivity of LSCO.

In addition to the many technological applications of these materials, $LaCoO_3$ and other rare earth cobaltates are also of scientific interest because of the peculiar way their magnetic and electrical transport properties change with temperature.[26] Early work on $LaCoO_3$ established the existence of a thermally induced spin transition from low spin Co to mostly high spin Co^{3+},[26] which has been used to explain the observed temperature dependence. Since then, many investigations have been carried out in order to elucidate how this spin transition takes place and the material evolves from semiconducting to metallic behavior as the temperature increases.[27]

Even though several workers have previously investigated the electrical conductivity and related properties of LSCO, very little is known about their thermal conductivity. The only article that discusses thermal properties of these materials is by Morgan,[28] who has predicted a relatively high thermal conductivity for LSCO. The present work was undertaken to investigate the thermal properties of LSCO and LSCNO.

II. SAMPLE PREPARATION

Samples of $La_{0.5}Sr_{0.5}Co_{1-x}Ni_xO_{3-\delta}$ (LSCNO) with x varied between 0 and 0.6 were prepared by a conventional solid-state ceramic route. High purity La_2O_3, Co_3O_4, NiO and $SrCO_3$ were weighed in the desired stoichiometric ratios, thoroughly mixed and ball milled for 24 h. The suspension was dried and calcined at 1100 °C for 4 h and the resulting calcined powder was ground well in an agate mortar with 3% polyvinyl alcohol added as binder, and again dried and ground well. The fine powder so obtained was pressed into

---
[a)]Author to whom correspondence should be addressed; electronic mail: mailadils@yahoo.com

pellets of thickness of 1 and 10 mm diameter under a pressure of about 0.01 kbar. The pellets were then sintered at 1300 °C for 2 h. The samples were hand lapped and polished to a thickness of nearly 0.5 mm for photopyroelectric measurements.

Pure $La_{0.5}Sr_{0.5}CoO_{3-\delta}$ (LSCO) samples were also prepared by hot pressing at 1100 °C at a pressure of 1 kbar in the presence of an oxygen flow. Disks of thickness nearly 1 mm were cut with a slow speed diamond wheel saw. They were then hand lapped and polished to a thickness of approximately 0.5 mm for the measurements reported in this work.

III. EXPERIMENTAL DETAILS

The photopyroelectric (PPE) technique has been used to determine the thermal parameters of the samples. A 120 mW He–Cd laser of wavelength 442 nm was used as the optical heating source with its intensity modulated by a mechanical chopper. A polymer polyvinylidene fluoride film of thickness 28 μm, with a Ni–Cr coating on both sides, was used as the pyroelectric detector, with a pyroelectric coefficient $p = -25 \times 10^{-6}$ C/m^2 K. The output signal was measured using a dual phase lock-in amplifier. The modulation frequency was maintained above 40 Hz to ensure that the detector, the sample, and the backing medium were thermally thick during the measurements. More details of the experimental setup are given in Ref. 29. The thermal thickness of LSCO and LSCNO samples has been verified by plotting the PPE amplitude and phase with frequency at different temperatures between room temperature and 180 K.

Measurement of the PPE signal phase and amplitude enables one to determine the thermal diffusivity α (defined as $k/\rho c_p$, where k is the thermal conductivity, ρ is the density, and c_p is the heat capacity of the sample) and the thermal effusivity e [defined as $\sqrt{(k\rho c_p)}$], respectively.[29] The k and c_p of the samples are determined from the measured values of α and e and the density ρ, which was determined by the Archimedes method. The experimental setup was calibrated by making measurements on a reference sample such as copper, as already reported earlier.[29] Measurements as a function of temperature were made during the heating cycle at a heating rate of approximately 0.5 K/min and data were collected every 1 K, and at smaller intervals near the M-I transition temperature. The temperature was measured with a platinum resistance sensor placed close to the sample inside the measurement chamber.

IV. RESULTS

Figure 1 shows the variation of PPE amplitude and phase with temperature for LSCO. It is seen that the PPE amplitude decreases monotonically with increase in temperature. The PPE phase also behaves in a similar manner, with a gradual decrease in its value with increase in temperature. No marked anomaly is observed in either the PPE amplitude or phase as the temperature is varied from about 160 K to room temperature.

Figure 2 shows the variation of thermal diffusivity and effusivity of LSCO with temperature. It is seen that thermal
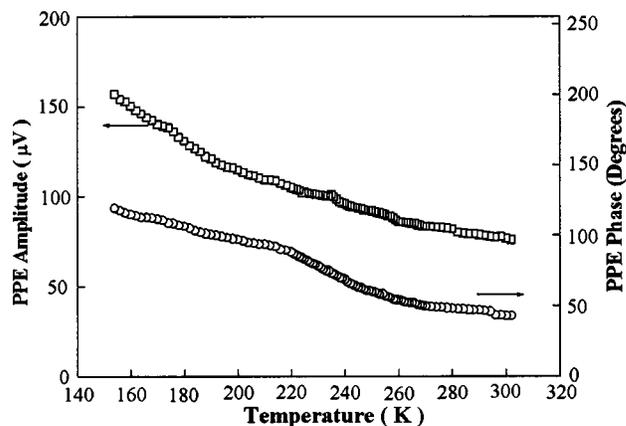

FIG. 1. Variation of PPE amplitude and phase with temperature for $La_{0.5}Sr_{0.5}CoO_{3-\delta}$.

diffusivity shows a gradual decrease with temperature, with no anomaly seen at any temperature. Since the thermal diffusivity is directly proportional to PPE phase, the variation of α with temperature is similar to the corresponding variation in PPE phase. Thermal effusivity also shows a gradual increase from 160 K up to room temperature. The nature of the variation of these two parameters with temperature indicates that no transition of any kind occurs for LSCO, with the sample showing pure metallic behavior throughout the scanned temperature range.

Figure 3 shows the variation of thermal conductivity and heat capacity of LSCO with temperature. It is seen that thermal conductivity shows a variation similar to the thermal diffusivity variation, whereas heat capacity increases with temperature. The variation of thermal conductivity with temperature highlights the metallic nature of the LSCO sample with no anomaly seen between 160 and 300 K.

In order to understand the effect of Ni doping on the thermal properties of LSCO, we have measured the density and thermal parameters of the $La_{0.5}Sr_{0.5}Co_{1-x}Ni_xO_{3-\delta}$ system with $x = 0.0$, 0.1, 0.2, 0.4, 0.5 and 0.6. Figure 4 shows the variation of the density of LSCNO samples as a function of Ni concentration. It may be noted that the density increases with Ni content. Figure 5 shows the variation of ther-
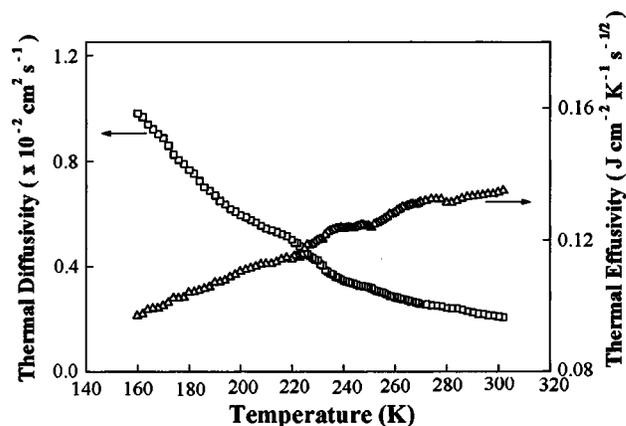

FIG. 2. Variation of thermal diffusivity and thermal effusivity with temperature for $La_{0.5}Sr_{0.5}CoO_{3-\delta}$.

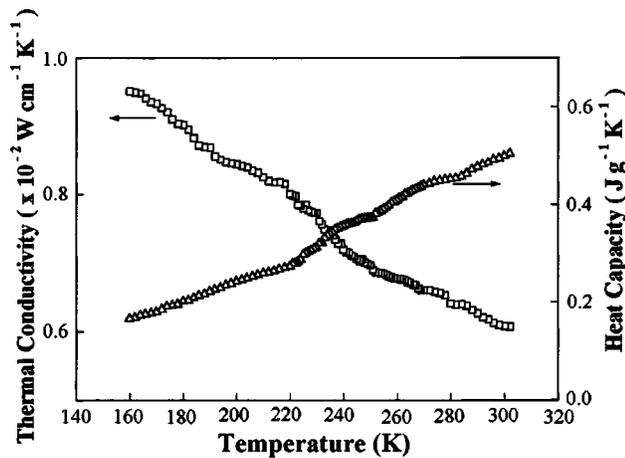FIG. 3. Variation of thermal conductivity and heat capacity with temperature for $La_{0.5}Sr_{0.5}CoO_{3-\delta}$.

FIG. 5. Variation of thermal diffusivity and thermal effusivity with Ni content for the $La_{0.5}Sr_{0.5}Co_{1-x}Ni_xO_{3-\delta}$ system at 300 K.

mal diffusivity and thermal effusivity with Ni concentration for the LSCNO system at room temperature. It is seen that thermal diffusivity increases monotonically with Ni content. Thermal effusivity also increases with Ni content up to $x = 0.4$, but beyond this doping level, it decreases gradually with Ni content.

Figure 6 shows the variation of thermal conductivity and heat capacity of the LSCNO system with Ni concentration. Unlike thermal diffusivity, which shows a gradual increase with composition, thermal conductivity shows a more rapid increase up to $x = 0.4$ and thereafter its value is almost constant. Heat capacity behaves in a similar manner. It is obvious from Fig. 6 that thermal conductivity increases by nearly a factor of 3 and heat capacity almost doubles as the Ni content is increased from $x = 0$ to $x = 0.4$

In order to study the temperature dependence of the thermal properties of LSCNO, we have carried out PPE measurements on all the samples from 160 to 300 K. The PPE amplitude and phase have been measured as a function of temperature and the variations are found to be similar to those shown in Fig. 1 for undoped LSCO. Figure 7 shows the
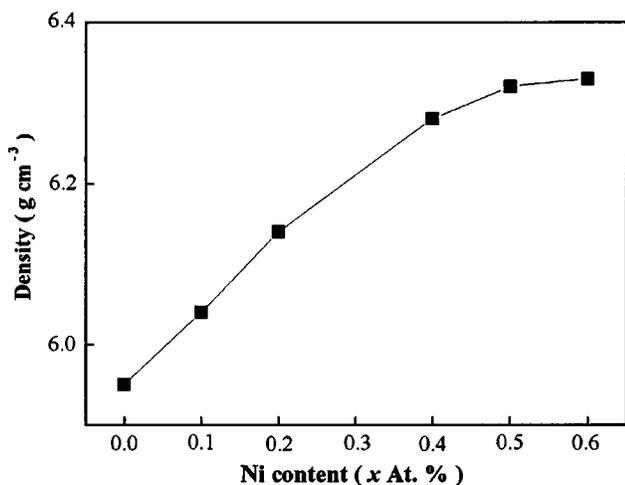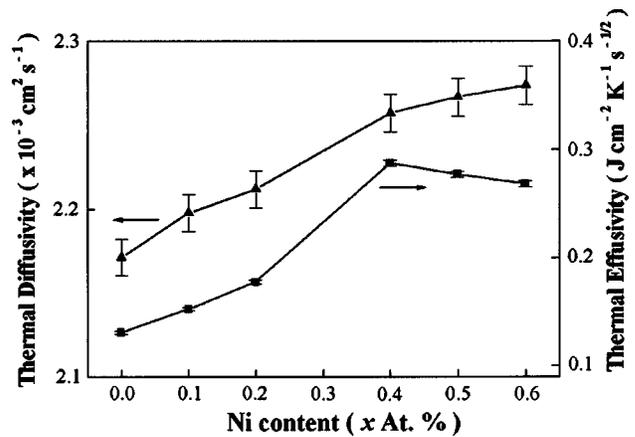
variation of thermal diffusivity and thermal effusivity with temperature for the $La_{0.5}Sr_{0.5}Co_{0.6}Ni_{0.4}O_{3-\delta}$ sample. Similar to the undoped LSCO sample, the thermal diffusivity decreases with temperature while thermal effusivity increases. All other samples show similar variations with temperature. Compared to LSCO, the values of α are increased significantly for the Ni doped samples at all temperatures at which measurements have been carried out. The thermal effusivity of the LSCNO samples also shows a corresponding increase at all temperatures compared to LSCO.

Figure 8 shows the temperature variation of thermal conductivity and heat capacity of the $La_{0.5}Sr_{0.5}Co_{0.6}Ni_{0.4}O_{3-\delta}$ sample. The variations of both k and c_p are similar to that of the parent sample $La_{0.5}Sr_{0.5}CoO_{3-\delta}$. As for α, the value of k increases substantially upon Ni doping. All the other samples with different Ni concentrations show similar variations in accordance with the variations shown in Fig. 6. The variation of thermal conductivity with temperature indicates that all of the Ni substituted samples exhibit metallic behavior in the temperature range under consideration.

PPE measurements have also been carried out on the LSCO samples prepared by hot pressing. The corresponding variations of thermal diffusivity and thermal effusivity deter-

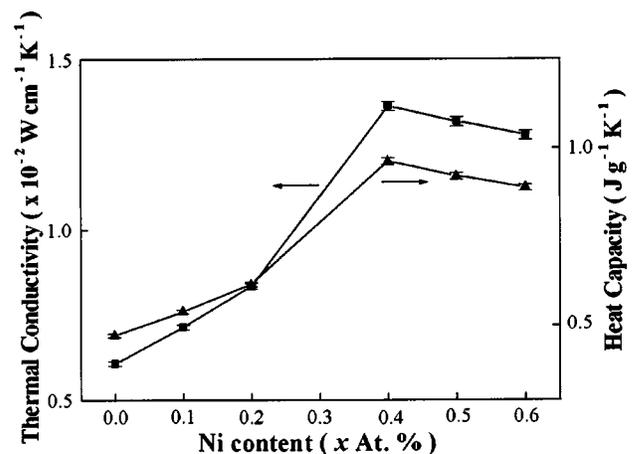FIG. 4. Variation of density with Ni content for the $La_{0.5}Sr_{0.5}Co_{1-x}Ni_xO_{3-\delta}$ system.

FIG. 6. Variation of thermal conductivity and heat capacity with Ni content for the $La_{0.5}Sr_{0.5}Co_{1-x}Ni_xO_{3-\delta}$ system at 300 K.
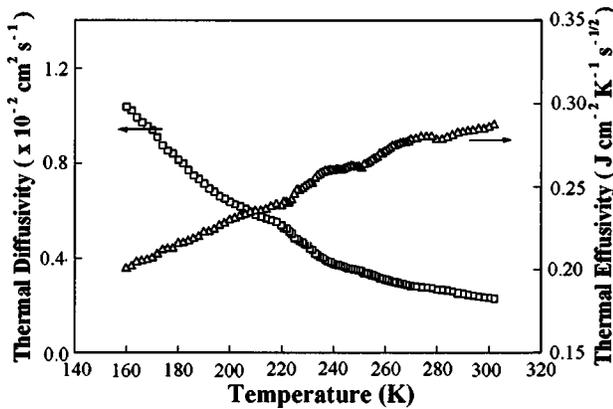
FIG. 7. Variation of thermal diffusivity and thermal effusivity with temperature for the $La_{0.5}Sr_{0.5}Co_{0.6}Ni_{0.4}O_{3-\delta}$ system.

FIG. 9. Variation of thermal diffusivity and thermal effusivity with temperature for hot pressed $La_{0.5}Sr_{0.5}CoO_{3-\delta}$.

mined from the PPE phase and amplitude values are shown in Fig. 9. The thermal conductivity and heat capacity have been evaluated from the thermal diffusivity and effusivity values and are plotted against temperature in Fig. 10. As can be noted from Figs. 9 and 10, all the thermal parameters undergo anomalous changes at around 240 K. As is evident from Fig. 10, thermal conductivity increases with temperature up to 240 K and beyond this it decreases with temperature. Based on this behavior it may be concluded that the material exhibits insulator-type behavior below 240 K and metal-type behavior above this temperature. The material thus exhibits an insulator-metal transition at around 240 K.

V. DISCUSSION OF RESULTS

The observed variation of the thermal parameters for the LSCO system can be explained as follows. In $LaCoO_3$, all the cobalt ions are in the diamagnetic low spin configuration at very low temperatures. The low spin Co^{III} ($t_{2g}^6 e_g^0, {}^1A_{1g}$) is, however, more stable with respect to the high spin Co^{3+} ($t_{2g}^4 e_g^2, {}^5T_{2g}$) state by only about 0.05 eV. With increasing temperature, the Co^{III} ions transform to Co^{3+}. Raccah and Goodenough[30] have identified a symmetry change from $R\bar{3}c$ to $R\bar{3}$ after this ordering and also observed a transition
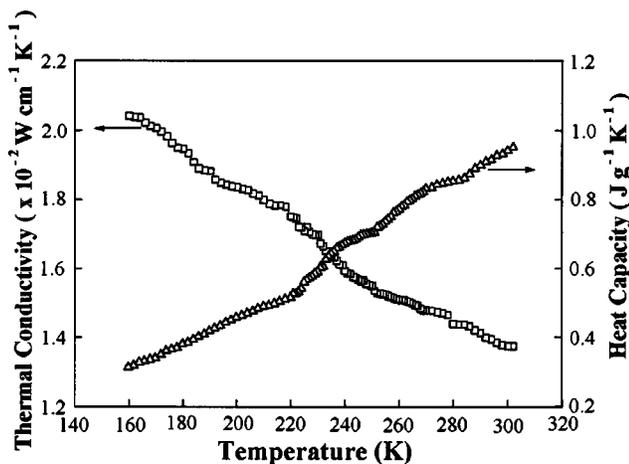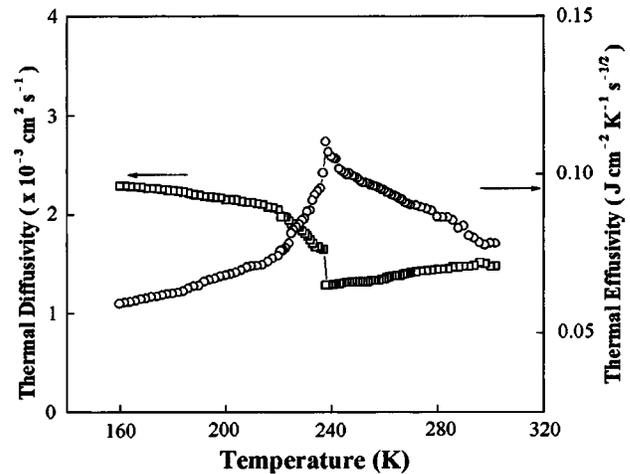
due to delocalization of the e_g electrons (localized at lower temperatures at high-spin Co^{3+} ions) to σ^*-band electrons at 1210 K. Beyond this $e_g - \sigma^*$ transition, $LaCoO_3$ becomes metallic.

Substitution of Sr^{2+} for La^{3+} in $LaCoO_3$ leads to high electrical conductivity and antiferromagnetic exchange interactions. As x increases, LSCO evolves toward a ferromagnetic intermediate spin state with σ^* electrons.[31] Bahadur *et al.*[32] have reported Mössbauer results supporting the intermediate spin state for the ferromagnetic regions of their samples. According to early literature, the $x = 0.5$ composition is a good conductor (resistivity $\rho < 10^{-4}$ Ω cm) and has a metallic-type temperature coefficient. In addition, it is ferromagnetic. Previous studies on LSCO have led to the suggestion that in the doped samples, paramagnetic La^{3+} regions coexist with ferromagnetic Sr^{2+} rich clusters in the same crystallographic phase, the ferromagnetic component increasing with x.[32]

The ferromagnetism observed in the LSCO system could be due to one of the following three mechanisms: (i) ordering of high spin and low spin cations through ferromagnetic super exchange between them via the intervening oxygen ion;[31] (ii) Zener double exchange;[33] and (iii) itinerant-

FIG. 8. Variation of thermal conductivity and heat capacity with temperature for the $La_{0.5}Sr_{0.5}Co_{0.6}Ni_{0.4}O_{3-\delta}$ system.

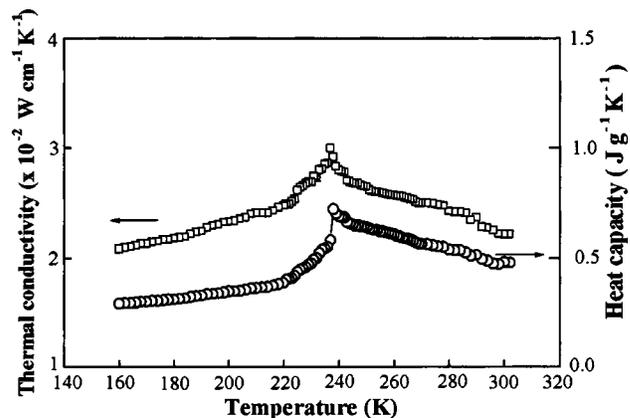FIG. 10. Variation of thermal conductivity and heat capacity with temperature for hot pressed $La_{0.5}Sr_{0.5}CoO_{3-\delta}$.

electron ferromagnetism.[30,31] The first mechanism, based on a localized electron model due to Anderson, was modified by Goodenough to account for the ferromagnetic interactions observed in the system. He showed that if octahedral site magnetic cations are located on opposite sides of a common anion, they interact ferromagnetically if one cation has completely empty e_g orbitals and the other has half filled e_g orbitals. However, this mechanism was abandoned later in favor of the itinerant electron ferromagnetism model.

As per the phase diagram for LSCO suggested by Goodenough,[31] $La_{0.5}Sr_{0.5}CoO_3$ belongs to the cluster glass phase. In this system, the double exchange between the trivalent and tetravalent cobalt spins and the exchange interaction between high spin Co^{4+} and low spin Co^{III} is considered to be ferromagnetic, whereas the super exchange interactions between high spin $(Co^{3+}-Co^{3+}, Co^{4+}-Co^{4+})$ are antiferromagnetic. The competition between the ferromagnetic and antiferromagnetic interactions along with the randomness lead to SG states observed for $0 \leq x \leq 0.18$. When the ferromagnetic exchange interactions just overcome the antiferromagnetic ones, the cluster glass phase appears with short range ferromagnetic ordering $(0.18 \leq x \leq 0.5)$.[31]

Earlier workers studied the effect of Co doping on the properties of the La–Ni–O system.[34] It was seen that while $LaNiO_3$ is metallic, $LaCoO_3$ is an insulator. At low temperature $(T < 200 \, K)$ Co^{3+} is in the low spin state (t_{2g}^6, e_g^0), the conduction band σ^* formed by the e_g state and oxygen p orbitals is empty, and the t_{2g} band is full. At higher temperatures $(T > 200 \, K)$ the Co ion undergoes a transition to a high spin state $(t_{2g}^4 e_g^2)$, which populates the σ^* band and the conductivity increases. Co also introduces disorder in the band structure due to the difference in the $3d$ levels $[E^{3d}(Co) - E^{3d}(Ni) \cong 1 \, eV]$. Most probably, the M-I transition in this material occurs in the σ^* band. Previous studies on $LaNi_{1-x}Co_xO_3$ have shown that as x is increased, temperature coefficient of conductivity $d\sigma/dT$ (at room temperature) changes sign for $x = 0.4$, which corresponds to $n \cong 10^{22}/cm^3$. This electron concentration is estimated from the assumption that each Ni^{3+} contributes one electron to the conduction band. The thermal conductivity results obtained for the Ni-doped samples of this study also exhibit a similar pattern, with the thermal conductivity increasing up to $x = 0.4$ (corresponding to Co concentration of 0.6).

The hot pressed LSCO samples behave in a different manner. It is found that thermal effusivity, thermal diffusivity, thermal conductivity and heat capacity show a peak at about 240 K (see Figs. 9 and 10). Magnetic and transport measurements have shown a M-I transition at about 250 K in bulk LSCO samples.[35,36] Madhukar *et al.*[37] have observed a similar broad transition in the variation of resistivity with temperature over the range 200–250 K in thin films. They reported that the M-I transition depends on the oxygen content in the sample. Our results indicate that the sintering atmosphere and oxygen stoichiometry play a dominant role in bringing about M-I transition in this family of samples. In the present case, LSCNO ceramic samples were prepared by conventional solid-state ceramic route and LSCO hot pressing was done in the presence of oxygen. This may be the reason for the absence of M-I transition in conventionally prepared samples.

VI. CONCLUSIONS

Thermal parameters, viz., thermal diffusivity (α) thermal effusivity (e), thermal conductivity (K), and heat capacity (c_p) of $La_{0.5}Sr_{0.5}CoO_{3-\delta}$ have been measured between 160 and 300 K. It is seen that the system is metallic throughout the temperature range and we can state that no temperature-dependent M-I transition is observed in the samples prepared by conventional solid-state sintering. In order to analyze the effect of Ni doping on $La_{0.5}Sr_{0.5}CoO_{3-\delta}$, we have measured the composition dependence of α, e, K, and c_p. The thermal conductivity and heat capacity are found to increase with Ni content. We have also measured the temperature dependence of thermal conductivity and heat capacity on $La_{0.5}Sr_{0.5}Co_{1-x}Ni_xO_{3-\delta}$ samples. As with pure LSCO, the LSCNO samples prepared by the conventional method do not exhibit any temperature-dependent M-I transition. However, pure LSCO prepared by hot pressing in the presence of an oxygen flow at 1100 °C shows a clear M-I transition. This difference in properties is attributed to the difference in the oxygen content of this sample.

[1] T. Nakamura, M. Misono, and Y. Yoneda, Chem. Lett. 1589 (1981).
[2] J. O. M. Bockins and T. Ogawa, J. Electrochem. Soc. **131**, 290 (1984).
[3] J. M. Bouwmeester and A. J. Burgraaf, in *CRC Handbook of Solid State Chemistry* (CRC, Boca Raton, FL, 1997), p. 481.
[4] N. Iehsa, K. Fukuya, K. Matsuo, N. Horichi, and N. Karube, J. Appl. Phys. **59**, 317 (1986).
[5] J. Liu, C. He, G. Chen, and W. Su, J. Mater. Sci. **32**, 203 (1997).
[6] O. Yamamoto, Y. Takeda, R. Canno, and M. Noda, J. Solid State Ionics **22**, 241 (1987).
[7] J. B. Goodenough and R. Raccah, J. Appl. Phys. **36**, 1031 (1963).
[8] Y. Ohno, S. Nagata, and H. Sato, J. Solid State Ionics **3/4**, 439 (1981).
[9] R. Ramesh, A. Inam, and W. K. Chan, Appl. Phys. Lett. **59**, 3542 (1991).
[10] D. S. Aggarwal, A. M. Dhote, R. Ramesh, W. L. Warren, G. E. Pike, D. Dimos, M. V. Raymond, and J. T. Evans, Appl. Phys. Lett. **69**, 2540 (1996).
[11] R. Mahendiran and A. K. Raychaudhari, Phys. Rev. B **54**, 16044 (1996).
[12] G. Briceno, H. Chang, X. Sun, P. G. Schultz, and X.-D. Xiang, Science **270**, 273 (1995).
[13] L. L. Wang and J. Zheng, Phys. Rev. B **54**, 1153 (1996).
[14] G. H. Jonker and J. H. Van Santen, Physica (Amsterdam) **19**, 120 (1953).
[15] P. M. Raccah and J. B. Goodenough, J. Appl. Phys. **39**, 1209 (1968).
[16] J. T. Cheung, F. E. D. Morgan, D. H. Lowndes, X. Y. Zheng, and J. Breer, Appl. Phys. Lett. **62**, 2045 (1993).
[17] A. Chairamani, M. Mathew, and D. D. Sarma, Phys. Rev. B **46**, 9974 (1992).
[18] H. Obhayashi, T. Kudo, and T. Gejo, Jpn. J. Appl. Phys. **13**, 1 (1974).
[19] J. F. M. Callessan, R. M. Wolf, and D. M. De Veiraman, Thin Solid Films **69**, 212 (1993).
[20] F. Wang and L. Lapparun, J. Appl. Phys. **82**, 1293 (1987).
[21] R. Ramesh, J. Lee, T. Sands, V. G. Keramidas, and O. Auciello, Appl. Phys. Lett. **64**, 2511 (1994).
[22] N. Iehisa, K. Fukaya, K. Matsuo, N. Horiuchi, and N. Karube, J. Appl. Phys. **59**, 317 (1986).
[23] J. Mizusaki, Y. Mina, S. Yamahuchi, K. Fueki, and H. Tagawa, J. Solid State Chem. **80**, 102 (1989).
[24] R. W. Schwartz, M. T. Sebastian, and M. V. Raymond, Mater. Res. Soc. Symp. Proc. **623**, 365 (2000).

[25] R. W. Schwartz, M. T. Sebastian, M. Charoenwongsa, and H. Dobberstein, Mater. Res. Soc. Symp. Proc. **666**, F11.7.1 (2001).

[26] C. N. R. Rao, O. M. Prakash, D. Bahadur, P. Ganguly, and S. Nagabhushana, J. Solid State Chem. **22**, 353 (1977).

[27] A. Mineshige, M. Kobune, S. Fujii, Z. Ogumi, M. Inaba, T. Yao, and K. Kikuchi, J. Solid State Chem. **142**, 374 (1999).

[28] P. E. D. Morgan, J. Am. Ceram. Soc. **58**, 349 (1975).

[29] C. Preethy Menon and J. Philip, Meas. Sci. Technol. **11**, 1744 (2000).

[30] P. M. Raccah and J. B. Godenough, J. Appl. Phys. **39**, 13 (1968).

[31] B. Goodenough, J. Phys. Chem. Solids **6**, 287 (1958); Mater. Res. Bull. **6**, 967 (1971).

[32] D. Bahadur, S. Kollali, C. N. R. Rao, M. J. Patni, and C. K. Srivastava, J. Phys. Chem. Solids **40**, 981 (1979).

[33] C. L. Zener, Phys. Rev. **82**, 403 (1951).

[34] K. Sreedhar, J. M. Honig, M. Darwin, M. Mc Elfresh, P. M. Shand, J. Xu, B. C. Crooker, and J. Spalek, Phys. Rev. B **46**, 6382 (1992).

[35] M. A. Senaris-Rodriguez and J. B. Goodenough, J. Solid State Chem. **118**, 323 (1995).

[36] S. Mukherjee, R. Ranganathan, D. S. Anilkumar, and P. A. Joy, Phys. Rev. B **54**, 9267 (1996).

[37] S. Madhukar, S. Aggarwal, A. M. Dhote, R. Ramesh, A. Krishnan, D. Keeble, and E. Pointdexter, J. Appl. Phys. **81**, 3543 (1997).